Planet. Space. Sci., Vol. 39, No. 6, pp. 895–906, 1991
Printed in Great Britain

0032-0633/91 $3.00+0.00

A ROCKET TOMOGRAPHY MEASUREMENT OF THE N_2^+ 3914 Å EMISSION RATES WITHIN AN AURORAL ARC

I. C. McDADE†
Space Physics Research Laboratory, Department of Atmospheric, Oceanic and Space Sciences, University of Michigan, Ann Arbor, MI 48109, U.S.A.

and

N. D. LLOYD and E. J. LLEWELLYN
Institute of Space and Atmospheric Studies (ISAS), Department of Physics, University of Saskatchewan, Saskatoon, Sask., Canada S7N 0W0

(*Received in final form* 4 *December* 1990)

Abstract—A rocket tomography experiment designed to measure the two-dimensional distribution of the N_2^+ 3914 Å volume emission rates within an auroral arc is described. A simple filter photometer on board a sounding rocket, which was launched during the ARIES auroral campaign, was used to measure the 3914 Å auroral brightnesses at elevation angles ranging from 0° to 360° in the plane of the rocket trajectory. The measured auroral brightnesses have been tomographically inverted to recover the local 3914 Å volume emission rates as a function of both altitude and latitude within the arc. The tomographic inversion procedure, which is based upon a maximum probability algebraic reconstruction approach, is described and the implications of the results for studies of auroral excitation processes are briefly discussed.

1. INTRODUCTION

During February of 1984 a major international field campaign, known by the acronym ARIES and described in more detail by Vallance Jones *et al.* (1991), was carried out from northern Manitoba, Canada, to study auroral excitation processes. As part of this campaign a Black Brant sounding rocket, equipped with various particle detectors and optical instruments, was launched towards and over an East–West aligned auroral arc. A major goal of the rocket-borne experiments, and coordinated ground-based observations, was to obtain information about the internal structure of such an auroral form. In this paper we present the results of one of the rocket experiments which was designed to measure the volume emission rates of the $N_2^+(B^2\Sigma_u^+ - X^2\Sigma_g^+)$ first negative (0–0) band as a function of both altitude and latitude within the arc.

2. THE ROCKET OBSERVATIONS

The ARIES "B" rocket (*ADD VC*-10), from which the present observations were made, was launched from Churchill Rocket Range (58.7°N, 266.2°E) at 03:53:44 U.T. on 28 February 1984. The rocket was launched southwards over an East–West aligned auroral form along a trajectory that was nearly coincident with the local magnetic meridian. At 3:57:37 U.T. the vehicle reached its 203 km apogee 72 km downrange from the launch site. At an altitude of 75 km on the flight upleg a vehicle manœuvre was initiated to orientate the rocket roll axis so that it would be perpendicular to the horizontal and vertical components of the local magnetic field. The desired vehicle attitude was achieved, to a good approximation, at an altitude of 118 km and maintained throughout the rest of the flight until the rocket began to tumble upon re-entry at an altitude of ~70 km. During the period of controlled flight the rocket was spinning about the roll axis with a period of 0.405 s. The filter photometer used to make the N_2^+ 3914 Å measurements was a photon counting device of conventional design with a half-cone field of view of 2.5°. The photometer was mounted in a side-look configuration with its optical axis perpendicular to the rocket roll axis. During each rocket roll, therefore, the line of sight of the photometer essentially scanned through elevation angles ranging from 0° to 360° in a plane that was nearly coincident with the plane of the trajectory and perpendicular to the East–West aligned auroral form. The photometer counts were recorded at a frequency of 200 Hz (5 ms bins) and this resulted in a ±2.2° smear in the measured brightnesses; this smear was comparable to that of the photometer field of view. The filter transmission function was 50 Å wide

† Formerly also with ISAS, University of Saskatchewan.

(FWHM), peaked at 3915 Å and captured between 90 and 93% of the $N_2^+(B^2\Sigma_u^+ - X^2\Sigma_g^+)$ (0–0) band over the range of rotational temperatures expected at auroral altitudes. The sensitivity of the photometer was calibrated before the flight using a standard low brightness source; this procedure provided a calibration factor of 13 counts s^{-1} R^{-1} of $N_2^+(B^2\Sigma_u^+ - X^2\Sigma_g^+)$ (0–0) band emission. Unfortunately, a post-flight calibration check could not be performed because the instrument was seriously damaged upon re-entry and impact. However, a comparison of the measurements made along similar lines of sight from the ground and from the rocket indicates that the rocket photometer must have been approximately 3 times more sensitive during the flight than the calibration had suggested. Although no errors have been found in the original calibration calculations we have tentatively adopted a revised calibration factor of 39 counts s^{-1} R^{-1}.

The 3914 Å photometer provided good data from rocket altitudes of 180 km on the flight upleg to approx. 70 km on the downleg. For reasons discussed below, this paper will focus mainly on the measurements that were made between rocket altitudes of ~190 and ~80 km on the downleg of the flight. These data are summarized in Fig. 1 which shows a shifted stack plot of the measured brightnesses as a function of photometer elevation for a number of consecutive roll scans. Figure 1 illustrates that when the rocket was at 200 km most of the auroral emission originated from below the rocket in the northern and southern-nadir quadrants. As the rocket descended through the 200–140 km region one feature labelled N in Fig. 1 moved away from the nadir (elevation 270°), passed through the North horizontal viewing direction (elevation 180°) and finally merged with a broader feature apparently developing in the zenith (elevation 90°). During this period a more southerly feature (labelled S in Fig. 1) simply faded as the broad feature in the zenith developed. The elevations of the two other prominent features in Fig. 1, labelled A and B, varied only slightly during the flight; as the rocket descended feature A drifted slowly towards the North horizontal (elevation 180°) and feature B broadened and moved towards, and through, the South horizontal (elevation 360°). It will be demonstrated below that the features A and B in Fig. 1 arose from latitudinally-extended auroral, or nightglow, sources viewed in a limb-enhanced mode, and that the features N and S arose from the more localized auroral sources of 3914 Å emission.

Although it is not perhaps immediately apparent, the data shown in Fig. 1 do contain a great deal of information about the spatial distribution and temporal variations of the 3914 Å emission rates within the auroral arc. For example, if temporal variations are neglected, then a simple triangulation analysis, illustrated in Fig. 2, would suggest that the feature labelled S in Fig. 1 probably arose from a southerly auroral core at an altitude close to 130 km, and that the feature N in Fig. 1 arose from a more northerly core at higher altitude. In the following analysis we demonstrate how quantitative information about the spatial distribution and the temporal variations of the N_2^+ 3914 Å emission rates within the arc may be extracted from the observational data.

3. A TOMOGRAPHIC INVERSION OF THE ROLL SCAN MEASUREMENTS

Several tomographic inversion techniques have been developed to deal with the problem of recovering two-dimensional volume emission rate distributions from surface brightness measurements made under conditions similar to those of the ARIES rocket experiment. The most successful tomographic techniques fall into two main categories; those based on two-dimensional algebraic reconstruction and those based on two-dimensional filtered transform methods. An algebraic reconstruction technique was first applied to aeronomic observations by Thomas and Donahue (1977) in their analysis of *OGO*-6 satellite data and techniques based on filtered transform methods have been used in the analysis of *Atmospheric Explorer* satellite data (Solomon *et al.*, 1984, 1985, 1988). In the present work we have applied an algebraic reconstruction technique which allows for the Poisson noise associated with the photometer photon counting statistics. As with other algebraic reconstruction techniques, the relevant region of the atmosphere is divided into a number of volume elements. Within each element the photon emission rate is assumed to be uniform and isotropic, and the surface brightness observed in a particular direction is assumed to be the sum of the contributions from all elements which intersect the line of sight. The number of elements is chosen so that the problem is overdetermined, i.e. the number of elements for which volume emission rates are to be recovered is less than the total number of different line of sight observations. From a consideration of the changing viewing geometry during the flight a system of linear equations is generated from the observational data set. This system of equations, which will not necessarily be consistent because of noise in the photometric data, is "solved" in the present work using a maximum probability approach to provide a best estimate of the volume emission rate distribution.

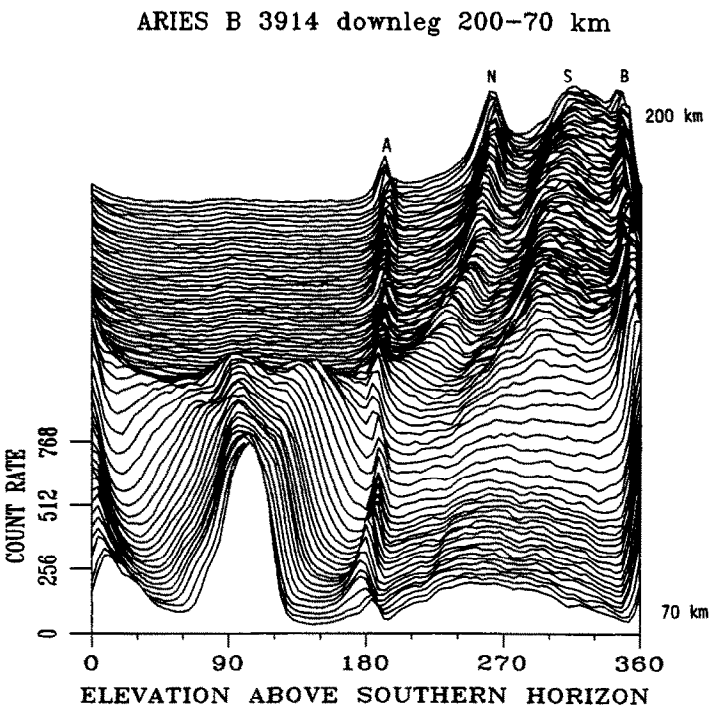

FIG. 1. A SEQUENCE OF PHOTOMETER SCANS ILLUSTRATING THE DATA OBTAINED FROM THE 3914 Å PHOTOMETER BETWEEN ALTITUDES OF 200 km (TOP) AND 70 km (BOTTOM) ON THE DOWNLEG OF THE ARIES "B" FLIGHT. To produce this plot the raw photometer counts were collected into equal elevation angle bins, then averaged over four consecutive scans and shifted in the ordinate for clarity. The count rate is expressed in counts per 5 ms integration period.

3.1. *Geometry of the contributing elements*

In order to achieve a successful inversion of the observations the array of volume elements that are allowed to contribute to the observed brightnesses must be carefully selected. For the analysis of the ARIES rocket data a primary array of 3075 elements was located within a rectangular grid which conservatively enclosed the main auroral form as determined from ground-based observations. This grid was divided into 75 columns and 41 rows of square elements with sides of 3 km. This grid lay in the plane of the rocket trajectory which was, to a good approximation, coincident with the plane of the photometer scan. The coordinate system of the grid was in the same frame as the rocket radar trajectory data, i.e. the rows and columns of the grid were parallel to the local horizontal and vertical directions at the launch site. Within this reference frame the primary grid enclosed the region of space lying between 80.5 and 203.5 km in altitude and extended from 18.5 km downrange to 243.5 km downrange of the launch site; this corresponds to approx. 2° of ground latitude. To extend this primary array to an altitude of ~215 km, where only weak emission is anticipated, an additional row of 75 rectangular elements each 12 km high and 3 km wide was placed on top of the primary grid. Since regions of space located well beyond the primary grid limits were viewed during each photometer scan, contributions from distant auroral or airglow sources of 3914 Å emission must be considered. In addition, the photometer line of sight intersected the solid Earth for many (~45%) of the observations made during each scan and so contributions from the ground and tropospheric albedo must also be taken into account.

Clearly, allowance for the more distant sources of 3914 Å emission cannot be made by simply extending the primary grid *ad infinitum* and a compromise has to be found between extending the grid and ensuring that the problem remains overdetermined. This compromise was achieved by assuming that the contributions from any distant sources could be modelled as having arisen from stratified airglow layers. The contributions from these layers were assigned to an additional 72 spatial elements. Each element was represented by a 3 km thick Earth-centred annulus; 36 of

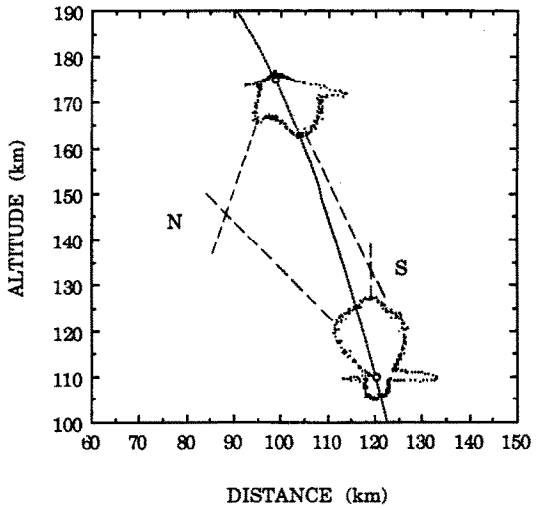

FIG. 2. POLAR PLOTS OF THE 3914 Å BRIGHTNESSES MEASURED DURING TWO SINGLE PHOTOMETER SCANS MADE AT 3:58:56 AND 3:59:58 U.T. WHEN THE ROCKET WAS AT ALTITUDES OF ~175 AND ~110 km, RESPECTIVELY.
The plots are centred on their respective positions along the flight trajectory which is shown by the dotted line. The intersections labelled "N" and "S" should qualitatively locate the strongest features in the spatial distribution of the 3914 Å emission.

these annuli were located to the North of the primary grid and 36 to the South. The altitudes represented by the annuli ranged from 80.5 to 188.5 km.

To allow for the albedo contributions it has been assumed that the snow-covered surface and lower atmosphere behaved like a Lambertian surface. The ground lying in the plane of the photometer scan between 5° North and 5° South of the centre of the primary grid was divided equally into 150 ground element bins; each ground bin was therefore approx. 7 km wide. It should be recognized that from an altitude of ~150 km the solid Earth horizon is displaced from the rocket position by ~12° in ground latitude. Consequently, during the flight the photometer did occasionally view regions of the ground lying outside the range of the ground array elements. However, because of the non-linear dependence of the sampled ground displacement upon photometer elevation, the vast majority of the observations which intersected the solid Earth did so within the ±5° ground element range.

The geometric distribution of the 3222 volume elements, for which emission rates are to be recovered, and the 150 ground elements, for which surface brightnesses are to be determined, are summarized in Fig. 3.

3.2. *The tomographic inversion algorithm and the recovered volume emission rates*

Under the algebraic reconstruction approach the surface brightness measured along a particular line of sight, identified by the index i, may be expressed as

$$O_i = \sum_j L_{ij} V_j + \sum_k \delta_{ik} B_k, \qquad (1)$$

where V_j is the emission rate within the volume element j; L_{ij} represents the path length of the line of sight i through the element j; B_k is the surface brightness of the ground element k; δ_{ik} is unity if the line of sight intersects the ground element k and zero otherwise. This formulation does not take into account the finite field of view of the photometer or the angular smearing resulting from the change in viewing direction during the photometer count integration period. Although allowance can be made for the finite field of view and angular smear, the physical dimensions of the chosen array elements are sufficiently large to allow these effects to be safely ignored for most viewing directions.

Using the rocket position data, available from the ground radar measurements, and the vehicle attitude information provided by the on-board gyro systems, the photometer line of sight at any particular time during the flight may be determined. From this the L_{ij} weighting factors and the values of the δ_{ik} in equation (1) may be calculated for each observation made during the flight. This results in a system containing tens of thousands of linear equations in the 3222 unknown V_js and 150 unknown B_ks. The tomographic inversion then reduces to the problem of solving this overdetermined set of equations. However, this formulation assumes that the V_js and B_ks remained constant during the time taken to acquire all of the observations. Coordinated ground-based measurements (Vallance Jones *et al.*, 1991) indicate that this was not strictly the case for the aurora under investigation. The requirement of time invariant V_js and B_ks could of course be satisfied by considering only the observations made during a small segment of the flight; however, such observations would have been made over a limited range of viewing positions and would therefore contain little tomographic information. To compromise this situation we first consider the data acquired between rocket altitudes of ~190 and ~80 km on the downleg of the flight. During this part of the descent 265 complete photometer scans were performed between 3:58:31 and 4:00:19 U.T. and 21,500 brightness measurements were made over a significant range of viewing positions. The resulting system of 21,500 equations in 3372 unknowns has been solved to provide an estimate

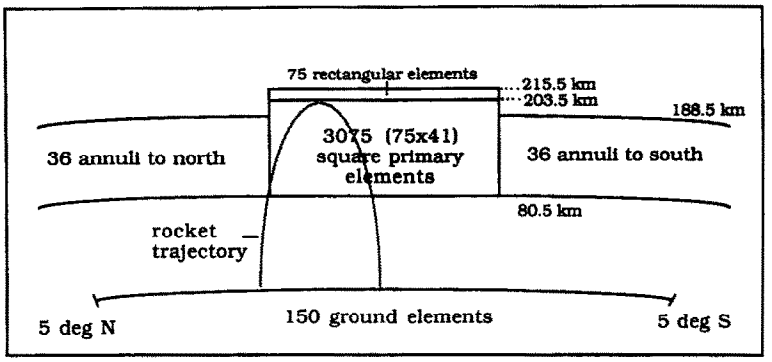

FIG. 3. A SUMMARY OF THE SPATIAL DISTRIBUTION OF THE 3222 VOLUME ELEMENTS AND 150 GROUND ELEMENTS CONSIDERED IN THE TOMOGRAPHIC INVERSION.

of the mean distribution of the 3914 Å volume emission rates within the aurora during this time period.

The algorithm used to solve this system of linear equations is based upon a maximum probability approach which takes into account the Poisson noise associated with the photon counting statistics of the photometer. The algorithm and its implementation have been described in detail by Lloyd and Llewellyn (1989). Essentially, an arbitrary set of initial volume emission rates, V_js, and ground surface brightnesses, B_ks, is used along with equation (1) to calculate an expected brightness for each of the 21,500 different lines of sight along which measurements were made. Each of the expected brightnesses (expressed in units of counted photons per photometer integration period) is then compared with the corresponding measured brightness. Any discrepancy between the measured and expected counts is treated as having arisen from random fluctuations (Poisson noise) in the number of photons, P_{ij}, actually received from each element, j, along the line of sight, i. For an observation of O_i counts from n_i contributing elements there are $(n_i+O_i-1)!/\{(n_i-1)!O_i!\}$ different possible sets of P_{ij}s. However, these $(n_i+O_i-1)!/\{(n_i-1)!O_i!\}$ different permutations are not all equally probable and the most likely set of contributions, $P_{ij}^{\max}$, is found using equation (15) of Lloyd and Llewellyn (1989). For each observation a record is kept of how much each contributing V_j or B_k would have to be changed in order to make the expectation value of its contribution to observation i, $L_{ij}V_j$ or $\delta_{ik}B_k$, identical to its maximum likelihood contribution, $P_{ij}^{\max}$. When all 21,500 expected and measured brightnesses have been compared, each of the initial V_j and B_k values is changed by an amount corresponding to the mean value of its implied changes. For the ground surface brightnesses this adjustment is based upon a simple average and for the volume emission rates the adjustment is based upon a weighted mean of the implied changes using the pathlength of each observation i through the element j as the weighting factor. This adjustment procedure results in an improved estimate of the volume emission rates and ground surface brightnesses. This process is then repeated in an iterative manner until the set of V_j and B_k values converges. Using the 190–80 km data set the solution had essentially converged after the ninth iteration. The mean distribution of the 3914 Å volume emission rates thus obtained is shown in panel (A) of Fig. 4 which represents the two-dimensional distribution of emission that would be most consistent with the observations if there were no temporal variations during the data acquisition period. It is clear from the contours shown in Fig. 4A that the volume emission rates in elements that lie along the parabola of the rocket trajectory are slightly enhanced or depleted relative to their nearest neighbours with which they should be highly correlated. This slight distortion along the trajectory may be suppressed by resetting the volume emission rates of each of the on-trajectory elements to the mean of their two nearest horizontal neighbours. The mean distribution obtained after resetting the on-trajectory elements is shown in panel (B) of Fig. 4.

Clearly, the distributions of 3914 Å emission shown in Fig. 4 are quite consistent with the qualitative expectations discussed in Section 3. The arc exhibits a primary core at an altitude of $\sim$130 km located $\sim$120 km downrange from the launch site, a secondary core is to be found some 30 km to the North at an altitude of $\sim$140 km. The contour lines are clearly more closely spaced below the peak emission than above it—as would be expected for the auroral 3914 Å emission—and the adopted primary grid does appear to enclose most of the auroral form. The small

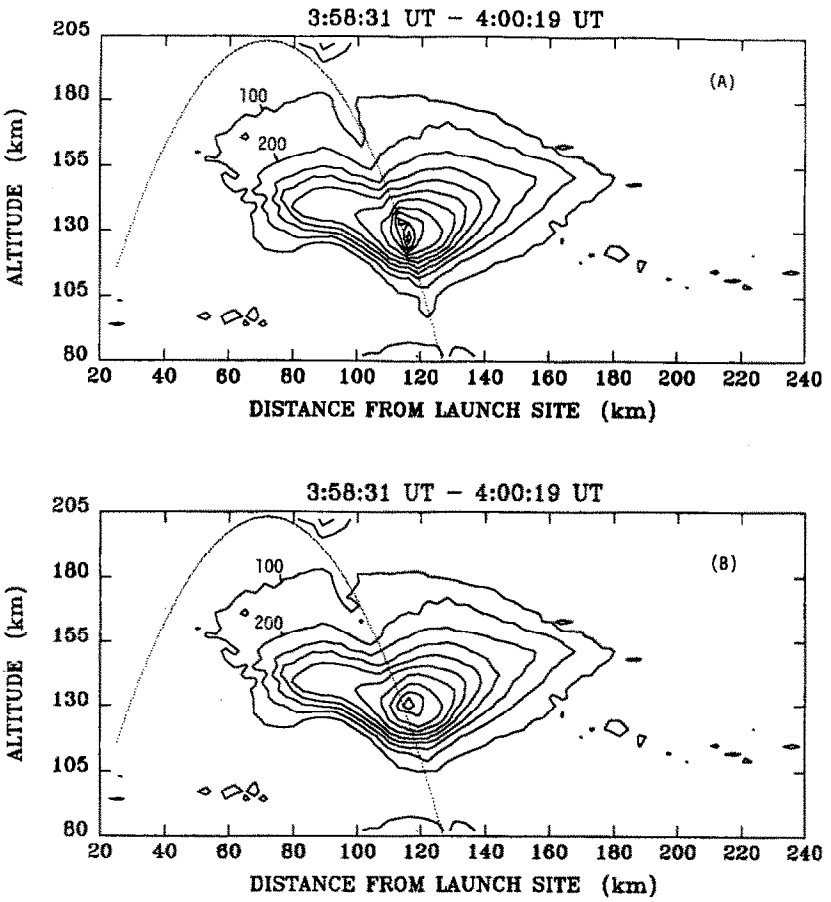

FIG. 4. (A) THE DISTRIBUTION OF 3914 Å EMISSION OBTAINED AS DESCRIBED IN THE TEST FROM AN INVERSION OF THE OBSERVATIONS MADE BETWEEN 3:58:31 AND 4:00:19 U.T.
The recovered N_2^+ 1N (0–0) band volume emission rate contours are drawn at equal intervals of 100 photons cm^{-3} s^{-1}. The dotted curve shows the rocket trajectory. (B) Same as shown in panel (a) with the emission rates along the trajectory modified as described in the text.

region of enhanced emission close to the rocket trajectory along the upper boundary of the grid may be real but a similar enhancement of the emission rates along the lower boundary of the grid below the main auroral core is more likely to be an artifact.

As discussed above, the coordinated ground-based measurements (Vallance Jones *et al.*, 1991) did indicate that there were temporal variations in the aurora as the rocket descended through the 190–80 km region. To assess the possible impact that these temporal variations may have had on the recovered distribution it is instructive to compare a number of actual photometer scans with scans reconstructed from the mean distribution for the 3:58:31–4:00:19 U.T. period. In Fig. 5 we show the measured and reconstructed brightnesses for scans performed at 3:58:56, 3:59:33 and 3:59:58 U.T. when the rocket was at 175, 140 and 110 km, respectively. Although the mean distribution does reproduce fairly well the qualitative and quantitative aspects of the scans made at these particular times, some discrepancies do exist between the measured and reconstructed brightnesses. For example, the brightness measured at a photometer elevation of 300° from 175 km is less than the brightness expected from the mean distribution which suggests that the southern core was somewhat weaker earlier in the flight.

In an attempt to allow for temporal variations in the aurora we have investigated the possibility of using the mean distribution derived from the 190–80 km data set as the starting point for a number of independent inversions based on sets of observations made

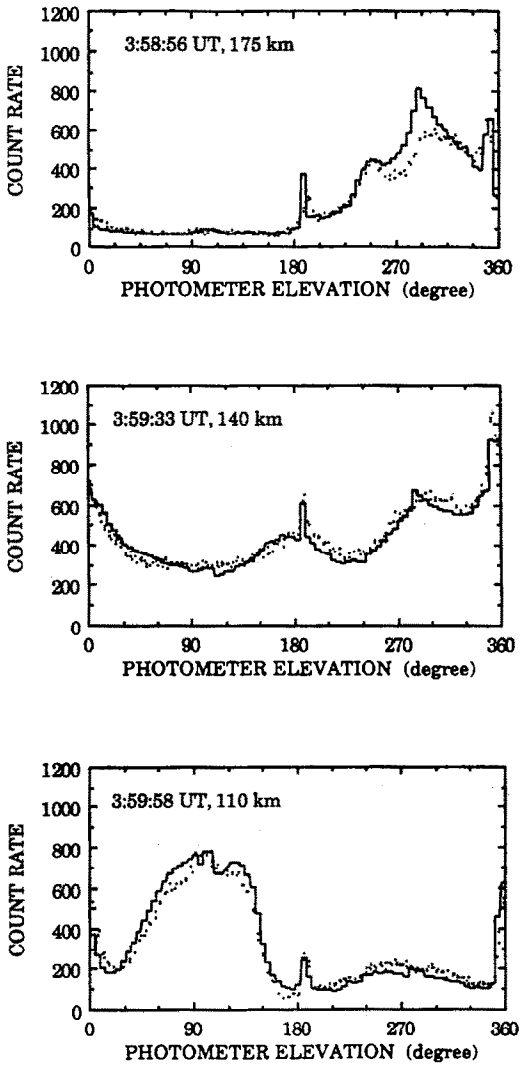

FIG. 5. THE MEASURED BRIGHTNESSES (DATA POINTS) AND THE BRIGHTNESSES RECONSTRUCTED FROM THE DISTRIBUTION OF FIG. 4B (HISTOGRAMS) FOR THE PHOTOMETER SCANS MADE AT 3:58:56, 3:59:33 AND 3:59:58 U.T. WHEN THE ROCKET WAS AT 175, 140 AND 110 km, RESPECTIVELY.
The data points represent the observations made during 1 s or approx. 2.5 rolls. The count rate is expressed in counts per 5 ms integration period.

over smaller time intervals. For example, if we use the mean distribution shown in Fig. 4 for the initial set of V_j and B_k values and apply the inversion algorithm to only the 15 seconds of observations centred on the rocket altitude of 175 km the distribution shown in Fig. 6 is obtained. Using this approach the solution had basically converged after three or four iterations. The distribution of Fig. 6 does provide an improved fit to the observations centred on the rocket altitude of 175 km (see Fig. 7) and indicates that the volume emission distribution during the 3:58:48–3:59:03 U.T. period had a stronger northern core and a weaker southern core than the distribution shown in Fig. 4. The distributions, and scan reconstructions, obtained in a similar manner using 15 s of observations centred on rocket altitudes of 140 and 110 km are shown in Figs 8–11. Here again the approach results in better agreement between the measured and reconstructed brightnesses and confirms that the northern core weakened and the southern core intensified during the rocket's descent.

Although the temporal evolution of the aurora, implied by Figs 6, 8 and 10, is quite consistent with the information available from the ground-based observations (Vallance Jones *et al.*, 1991), it is difficult to assess the level of confidence that should be placed in the recovered volume emission rate distributions. However, an examination of the ground surface brightnesses that were recovered along with the volume emission rates does lend support to their validity. When considering the recovered ground surface brightnesses we should point out that these quantities are obtained from the inversion algorithm independently of the volume emission rates, i.e. the ground brightnesses, or B_ks, are free parameters that are not in any way constrained to the values of the overhead V_js. Physically, however, the ground surface brightnesses are determined by the distribution of volume emission rates. Consequently, a comparison of the recovered V_js and B_ks provides an important means of testing the reliability of the entire inversion procedure.

The relationship between the brightness of a scattering surface, assumed in this case to be Lambertian, and the distribution of luminosity above it has been considered within the context of auroral photometry by Hays and Anger (1978). With the assumption that the aurora under investigation extended uniformly in the East–West direction, we have used the formulation described by Hays and Anger (1978) to calculate the ground surface brightnesses that would be expected to accompany the 3914 Å volume emission rate distribution shown in Fig. 10. The distribution of ground surface brightnesses thus obtained, assuming initially a 3914 Å surface albedo of unity for all ground elements, is similar in shape to the ground brightness distribution that was recovered along with the volume emission rates of Fig. 10. The normalization factor required to match these two distributions, as shown in Fig. 12, corresponds to an effective 3914 Å albedo of 0.65. This ground albedo compares quite favourably with the value of 0.8 usually adopted for this spectral

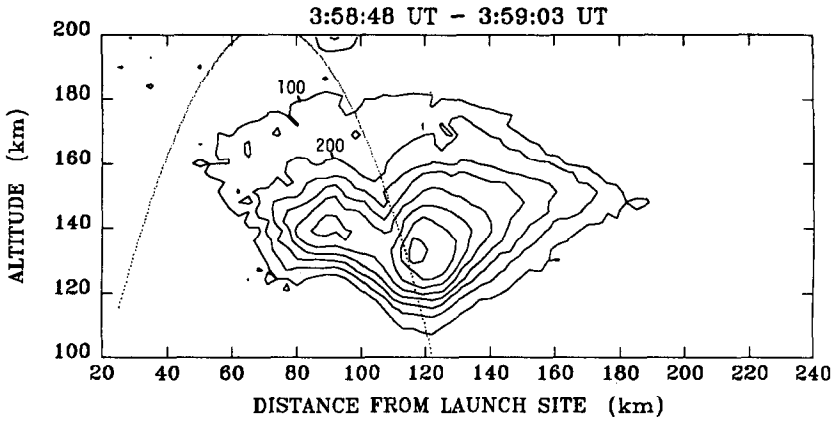

FIG. 6. THE DISTRIBUTION OF 3914 Å EMISSION OBTAINED AS DESCRIBED IN THE TEXT FROM AN INVERSION OF THE OBSERVATIONS MADE DURING THE 15 s INTERVAL CENTRED ON 3:58:56 U.T. WHEN THE ROCKET WAS AT AN ALTITUDE OF 175 km.
The recovered N_2^+ 1N (0–0) band volume emission rate contour lines are drawn at intervals of 100 photons cm^{-3} s^{-1}. The dotted curve shows the rocket trajectory.

region (Hays and Anger, 1978). Further evidence to support the validity of the recovered volume emission rates emerges from an inspection of the volume emission rates assigned, by the inversion procedure, to the northern and southern arrays of stratified layers.

In Fig. 13 we show the volume emission rates assigned to the stratified arrays by the inversion of the 15 s of observations centred on a rocket altitude of 110 km. The bulk of the 3914 Å emission originating from the northern limb is restricted to a narrow layer lying between altitudes of 80 and 100 km. In contrast, the emission originating from the southern limb is much stronger and shifted to altitudes that are more typical of auroral emissions. This marked North/South asymmetry is quite typical of what would be expected in the vicinity of a discrete auroral arc. Equatorward of discrete arcs a number of diffuse auroral forms, distributed over several degrees of latitude, are usually observed. To the North the level of optical auroral activity is usually much weaker. It should also be noted that the shape of the emission profile recovered for the northern stratified layers closely

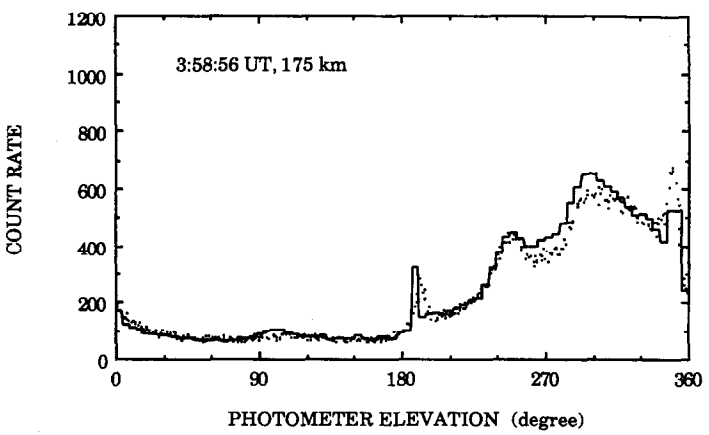

FIG. 7. THE MEASURED BRIGHTNESSES (DATA POINTS) AND THE BRIGHTNESSES RECONSTRUCTED FROM THE DISTRIBUTION OF FIG. 6 (HISTOGRAM) FOR A PHOTOMETER SCAN MADE AT 3:58:56 U.T. WHEN THE ROCKET WAS AT AN ALTITUDE OF 175 km.
The data points represent the observations made during a 2 s interval centred on the time of interest. The count rate is expressed in counts per 5 ms integration period.

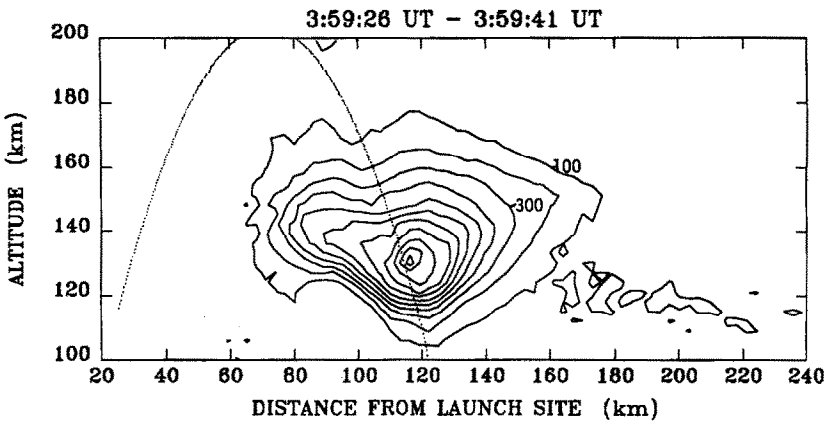

FIG. 8. THE DISTRIBUTION OF 3914 Å EMISSION OBTAINED AS DESCRIBED IN THE TEXT FROM AN INVERSION OF THE OBSERVATION MADE DURING THE 15 s INTERVAL CENTRED ON 3:59:33 U.T. WHEN THE ROCKET WAS AT AN ALTITUDE OF 140 km.
The recovered N_2^+ 1N (0–0) band volume emission rate contour lines are drawn at intervals of 100 photons cm^{-3} s^{-1}. The dotted curve shows the rocket trajectory.

resembles a quiescent O_2 nightglow emission profile (Murtagh *et al.*, 1986a,b). It is tempting to suggest, therefore, that the northern limb emission is due to the O_2 nightglow rather than auroral N_2^+. The 3914 Å photometer filter would have captured only a small fraction of the total O_2 nightglow emission, but the relatively strong (5–3) and (3–2) bands of the $O_2(A'^3\Delta_u \rightarrow a^1\Delta_g)$ Chamberlain system fall within the passband of the 3914 Å filter. We have considered the filter capture functions for the various O_2 nightglow systems and find that for typical nightglow intensities of 500, 100 and 200 R in the Herzberg I, Herzberg II and Chamberlain systems (Murtagh *et al.*, 1986a,b), the total zenith intensity captured by the photometer would have been ~20 R. The northern limb emission profile shown in Fig. 13 represents a captured zenith intensity of ~25 R. It seems likely, therefore, that most of the northern limb emission did arise from the O_2 Chamberlain band system. It may at first seem surprising that a nightglow profile could have been resolved, or partially resolved, from airglow limb scan observations made with a photometer with a 2.5°

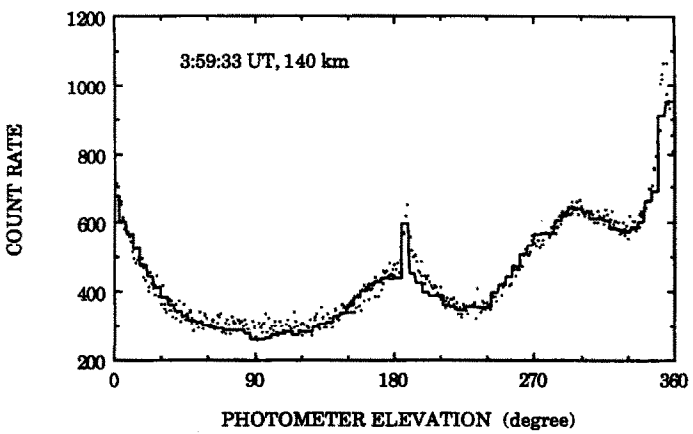

FIG. 9. THE MEASURED BRIGHTNESSES (DATA POINTS) AND THE BRIGHTNESSES RECONSTRUCTED FROM THE DISTRIBUTION OF FIG. 8 (HISTOGRAM) FOR A PHOTOMETER SCAN MADE AT 3:59:33 U.T. WHEN THE ROCKET WAS AT AN ALTITUDE OF 140 km.
The data points represent the observations made during a 2 s interval centred on the time of interest. The count rate is expressed in counts per 5 ms integration period.

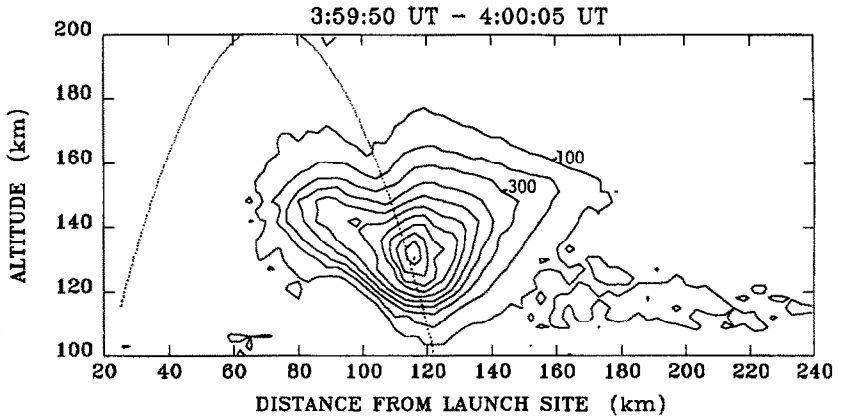

FIG. 10. THE DISTRIBUTION OF 3914 Å EMISSION OBTAINED AS DESCRIBED IN THE TEXT FROM AN INVERSION OF THE OBSERVATIONS MADE DURING THE 15 s INTERVAL CENTRED ON 3:59:58 U.T. WHEN THE ROCKET WAS AT AN ALTITUDE OF 110 km.
The recovered N_2^+ 1N (0–0) band volume emission rate contour lines are drawn at intervals of 100 photons cm^{-3} s^{-1}. The dotted curve shows the rocket trajectory.

field of view. However, the rocket did pass through the airglow layer upon descent and the scans made late in the flight would have provided side look observations, etc. that the inversion algorithm would automatically deconvolve.

4. DISCUSSION AND CONCLUSIONS

The N_2^+ 3914 Å volume emission distributions obtained in the previous section for three selected times during the descent of the ARIES "B" rocket, represent a rather unique data base for investigations of auroral excitation processes. When considered along with the comprehensive energetic particle measurements that were made during the flight (Vallance Jones *et al.*, 1991) the data should allow various auroral models to be tested in a manner not usually afforded by a single rocket experiment. Conventional rocket auroral photometry experiments can only provide information about the excitation and ionization rates occurring along a single field line involving incident electrons with a particular energy spectrum—or

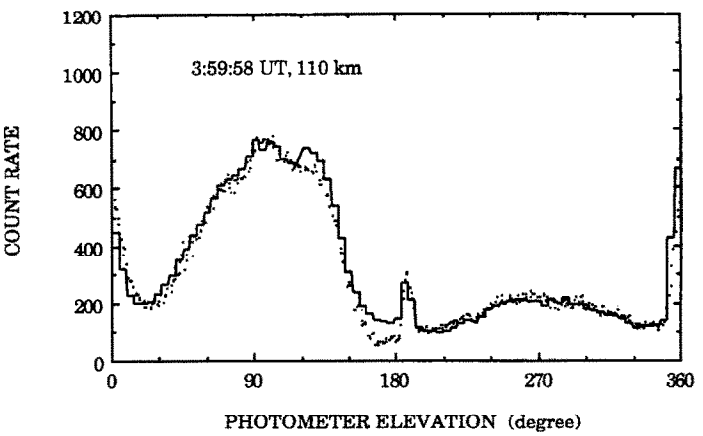

FIG. 11. THE MEASURED BRIGHTNESSES (DATA POINTS) AND THE BRIGHTNESSES RECONSTRUCTED FROM THE DISTRIBUTION OF FIG. 10 (HISTOGRAM) FOR A PHOTOMETER SCAN MADE AT 3:59:58 U.T. WHEN THE ROCKET WAS AT AN ALTITUDE OF 110 km.
The data points represent the observations made during a 2 s interval centred on the time of interest. The count rate is expressed in counts per 5 ms integration period.

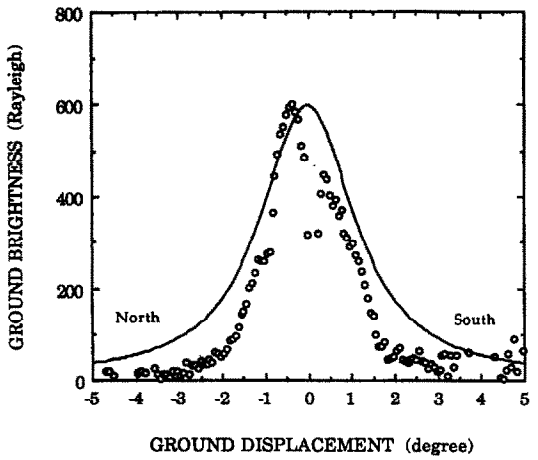

FIG. 12. THE GROUND SURFACE BRIGHTNESSES (CIRCLES) RECOVERED ALONG WITH THE VOLUME EMISSION RATES SHOWN IN FIG. 10 AND THE THEORETICAL GROUND BRIGHTNESSES (SOLID CURVE) CALCULATED AS DESCRIBED IN THE TEXT WITH AN EFFECTIVE 3914 Å ALBEDO OF 0.65.

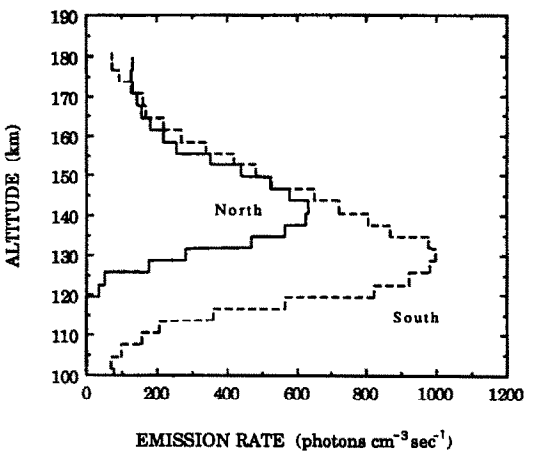

FIG. 14. N_2^+ 1N (0–0) BAND VOLUME EMISSION PROFILES EXTRACTED FROM THE DISTRIBUTIONS SHOWN IN FIGS 6 AND 8.
The profile labelled "North" corresponds to a field line passing through the rocket at ~180 km and close to the centre of the northern auroral core in Fig. 6. The profile labelled "South" corresponds to a field line passing through the rocket at ~130 km and close to the centre of the main auroral core in Fig. 8.

more strictly a number of field lines upon which the incident spectra and fluxes are assumed to be the same. The measured profiles can then only be compared with model expectations for that particular incident electron spectrum. In contrast, the results of the ARIES experiment will allow comparisons to be made with a number of profiles measured along field lines involving different incident spectra. An additional advantage of this approach is that the analysis of these essentially different precipitation events can be performed with the knowledge that they all occurred under otherwise identical atmospheric conditions.

Examples of the 3914 Å emission profiles that may be extracted from the recovered two-dimensional distributions are shown in Fig. 14. The profile labelled "North" in Fig. 14 is a slice through the distribution of Fig. 6 and corresponds to a field line passing through the rocket at ~180 km and close to the centre of the northern auroral core. The profile labelled "South" in Fig. 14 is a slice through the distribution shown in Fig. 8 and corresponds to a field line passing through the rocket at ~130 km and close to the centre of the southern auroral core. Clearly, the energy spectra of the electrons incident upon these two field lines must have been quite different. In a companion paper by Vallance Jones *et al.* (1991) these 3914 Å emission profiles are compared with theoretical profiles calculated using various auroral excitation models and the *in-situ* energetic particle measurements.

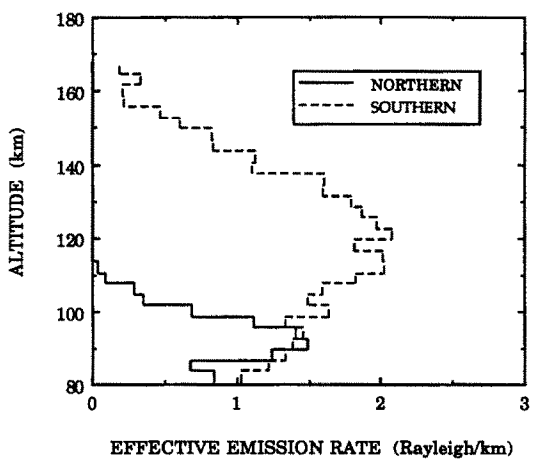

FIG. 13. THE VOLUME EMISSION RATES ASSIGNED TO THE NORTHERN AND SOUTHERN STRATIFIED LAYERS BY THE INVERSION OF THE OBSERVATIONS CENTRED ON 3:59:58 U.T.
The emission rates are expressed in terms of Rayleighs captured by the photometer.

Acknowledgements—The authors would like to thank Drs A. Vallance Jones and R. L. Gattinger for many valuable discussions and their encouragement to pursue the tomographic studies presented here. We also wish to express our gratitude to the National Research Council of Canada Space Division personnel, particularly Mr Hal Roberts, for their efforts to ensure the success of the ARIES campaign and the rocket launch. This work was supported at the University of

Michigan by internal funds from the Space Physics Research Laboratory and by the National Aeronautics and Space Administration grant NAG5-670. At the University of Saskatchewan the work was supported by Grants-In-Aid from the Natural Sciences and Engineering Research Council of Canada.

REFERENCES

Hays, P. B. and Anger, C. D. (1978) Influence of ground scattering on satellite auroral observations. *Appl. Opt.* **17**, 1898.

Lloyd, N. D. and Llewellyn, E. J. (1989) Deconvolution of blurred images using photon counting statistics and maximum probability. *Can. J. Phys.* **67**, 89.

Murtagh, D. P., McDade, I. C., Greer, R. G. H., Stegman, J., Witt, G. and Llewellyn, E. J. (1986a) ETON 4: an experimental investigation of the altitude dependence of the $O_2(A^3\Sigma_u^+)$ vibrational populations in the nightglow. *Planet. Space Sci.* **34**, 811.

Murtagh, D. P., Witt, G. and Stegman, J. (1986b) O_2-triplet emissions in the nightglow. *Can. J. Phys.* **64**, 1587.

Solomon, S. C., Hays, P. B. and Abreu, V. J. (1984) Tomographic inversion of satellite photometry. *Appl. Opt.* **23**, 3409.

Solomon, S. C., Hays, P. B. and Abreu, V. J. (1985) Tomographic inversion of satellite photometry. Part 2. *Appl. Opt.* **24**, 4134.

Solomon, S. C., Hays, P. B. and Abreu, V. J. (1988) The auroral 6300 Å emission: observations and modelling. *J. geophys. Res.* **93**, 9867.

Thomas, R. J. and Donahue, T. M. (1977) Analysis of *Ogo* 6 observations of the OI 5577Å tropical nightglow. *J. geophys. Res.* **77**, 79.

Vallance Jones, A., Gattinger, R. L., Creutzberg, F., Harris, F. R., McNamarra, A. G., Yau, A. W., McEwan, D. J., Llewellyn, E. J., Lummerzheim, D., Rees, M. H., McDade, I. C. and Margot-Chaker, J. (1991) Characterization and modelling of an evening auroral arc observed from a rocket and a ground-based line of meridian scanners. *Planet. Space Sci.* (submitted).